Statistical validation of structured population models for *Daphnia magna*

Kaska Adoteye[a,b], H.T. Banks[a,b], Karissa Cross[c], Stephanie Eytcheson[c], Kevin B. Flores[a,b], Gerald A. LeBlanc[c], Timothy Nguyen[b], Chelsea Ross[a], Emmaline Smith[b], Michael Stemkovski[c], Sarah Stokely[a]

[a]Center for Research in Scientific Computation
[b]Department of Mathematics
[c]Toxicology Program, Department of Biological Sciences
North Carolina State University, Raleigh, NC, United States

November 26, 2014

Abstract

In this study we use statistical validation techniques to verify density-dependent mechanisms hypothesized for populations of *Daphnia magna*. We develop structured population models that exemplify specific mechanisms, and use multi-scale experimental data in order to test their importance. We show that fecundity and survival rates are affected by both time-varying density-independent factors, such as age, and density-dependent factors, such as competition. We perform uncertainty analysis and show that our parameters are estimated with a high degree of confidence. Further, we perform a sensitivity analysis to understand how changes in fecundity and survival rates affect population size and age-structure.

Key Words: Sensitivity analysis; structured population model; uncertainty quantification; density-dependence; multi-scale data; *Daphnia magna*

1 Introduction

Structured population models (SPMs) are well characterized for describing aggregate ecological data across a wide variety of species [13, 17]. Numerous studies have exemplified the practical utility of SPMs in conservation biology [15, 20, 46, 47] and hazard assessments [45, 50] by making predictions of population decline or recovery. Importantly, SPMs have been used to analyze factors influencing the imperilment of endangered species populations [16, 25, 27, 29, 51].

The predictive value of a SPM, or of any mathematical model, relies on the degree of fidelity of the model to existing data and in the uncertainty in parameters estimated from that data. Several factors involving data information content can affect the uncertainty in parameters estimated for a structured population model. Beyond the usual issues in optimizing the measurement frequency, variance, and resolution of the structured variable (age/size), a central problem affecting SPM parameter uncertainty is that aggregate data may not support the simultaneous estimation of parameters describing multiple biological scales. This "individual dynamics/aggregate data" problem [9] arises due to the interrelation of individual dynamics and aggregate behavior described by SPMs. For example, the mathematical equations describing a fecundity rate in the model might involve a density-independent rate multiplied by a density-dependent rate. Since a lower density-independent rate can be compensated for by a higher density-dependent rate, the multiplication creates a correlation that contributes to a higher level of uncertainty when these rates are concurrently estimated.

An additional confounding factor in estimating parameters for SPMs is encountered when density-independent demographic rates are time- or age-dependent. For example, the rates describing fecundity and survival are known to vary with age in many species. In addition, these age-dependent rates may also be affected by exposure of the organism to exogenous chemicals or other stressful environmental conditions. Although SPMs can be easily modified to describe age-dependent demographic parameters, the accurate estimation of those parameters can be prohibited by practical limitations, e.g., computational tractability [3, 52]. Moreover, the individual dynamics/aggregate data problem is exacerbated because time-dependence is mathematically treated by extending a single parameter to a function described by several parameters.

One approach to redressing the "individual dynamics/aggregate data" problem is to collect, when feasible, demographic data from organisms grown in isolation. This data is then used to estimate density-independent parameters comprised in the demographic rates, which are then fixed in the population model. This enables the estimation of the remaining density-dependent parameters in the population model from longitudinal aggregate data. An added advantage to this approach is that age-dependent rates can also be estimated or directly represented by the collected organismal data, removing the rather complex problem of estimating these rates from aggregate data alone.

Here, we present this approach for estimating density- and age-dependent demographic

rates in SPMs for *Daphnia magna*. This species of water flea has been characterized by the National Institutes of Health as a model organism for biomedical research [36]. *D. magna* is also widely used in ecotoxicology to assess the hazard of exogenous chemicals, e.g., pesticides, on ecosystems [31, 32, 48, 49]. These assessments, however, have mainly focused on endpoints below the population level of biological organization, i.e., at the molecular, cellular, or organism levels. SPMs can be used to propagate organismal assessments to the population level, thereby enabling the causal association of organismal responses to ecosystem adversity.

Among the recent literature, several mathematical models were developed to describe the longitudinal dynamics of daphnid populations. Erickson, et al. [21], formulated a SPM to investigate the impact of stochastic fecundity and survival on the ability of their model to describe data from pesticide treated populations. Importantly, the model from this study was calibrated to data that only captured the early population growth phase of daphnids. Thus, it has not been determined whether a SPM with stochastic demographics can accurately describe the long-term dynamics of daphnid populations, which is qualitatively different from the early growth phase [42]. Preuss, et al. [42], validated an individual based model in order to predict the effect of variable algae concentration levels on daphnid population dynamics. Other recent efforts [18, 19, 22] to develop daphnid SPMs have focused on qualitative analysis of the general population dynamics rather than model validation.

Here, we collected both individual and population level data and developed multiple daphnid SPMs in order to test the importance of several biological assumptions. Specifically, we mathematically tested the validity of assuming a time-delay in density-dependent fecundity. We collected daily reproduction data on thirty daphnids to precisely investigate age-dependent fecundity rates for accurate representation in a SPM. We also validated a mathematical description of density-dependent survival and tested whether density-dependent fecundity and survival could be more accurately modeled as a function of total biomass rather than the total population size. Our investigation of delayed density-dependent fecundity is motivated by previous experimental evidence found in [23, 41]; we note that this assumption has not been tested in the context of SPMs in recent literature and with modern daphnid culture methodology. We also collected precise growth rate data on thirty daphnids (starting at within 2-hours of birth) to calibrate our age-structured observations of juvenile and adult daphnids. We employed quantitative model comparison techniques to assess the validity of our underlying assumptions. Finally, we performed quantitative sensitivity and uncertainty analyses on the SPM with the most accurate biological assumptions among the SPMs we considered.

2 Methods

2.1 Population models

Each model we describe in the sections below is a specification of the following structured population model:

$$\begin{bmatrix} p(t+1,1) \\ p(t+1,2) \\ p(t+1,3) \\ \vdots \\ p(t+1,i_{max}) \end{bmatrix} = \begin{bmatrix} a(t,1) & a(t,2) & a(t,3) & \dots & a(t,i_{max}) \\ b(t,1) & 0 & 0 & \dots & 0 \\ 0 & b(t,2) & 0 & \dots & 0 \\ \vdots & & \ddots & \dots & \vdots \\ 0 & 0 & 0 & \dots & b(t,i_{max}-1) \end{bmatrix} \begin{bmatrix} p(t,1) \\ p(t,2) \\ p(t,3) \\ \vdots \\ p(t,i_{max}) \end{bmatrix}. \quad (1)$$

The population is divided into one-day age classes, ranging from neonates at age $i = 1$ to a maximum lifespan at age $i = i_{max}$, where the number of daphnids of age i at a time t is $p(t, i)$. Here, we assume $i_{max} = 74$ based on our individual level experiments, and based on simulations of our models fit to experimental data, i.e., the maximum life span observed in the simulations was always less than 74 days. The fecundity of each age class i is given by $a(t, i)$ and the survival probability is given by $b(t, i)$.

We generated several models to investigate the importance of several density-dependent mechanisms in modeling *D. magna* populations. Significance of the different mechanisms was assessed by using statistical comparison tests between different models fit to the same structured population data. We specified the functional forms for $a(t, i)$ and $b(t, i)$ in equation (1) to generate four different structured population models for this assessment, which we refer to as models A through D (Table 1). The four models we consider are organized by the sequential generalization of the functional forms for fecundity and survival, i.e., models A and D have the least and most number of parameters, respectively.

2.1.1 Delayed density-dependent fecundity

To evaluate the importance of delayed density-dependent fecundity, we generated models A and B (Table 1) with parameters $\theta = (\mu, q)$ to be estimated. In model A, we assume density-dependent fecundity for all daphnid age classes. We used a functional form for fecundity that decreases with total population size $N(t)$ [26](see $a(t, i)$ in Table 1a). The strength of the density-dependent effect on fecundity is represented by the parameter q; the fecundity is density-independent when $q = 0$. Model A assumes a density- and age-independent survival probability, i.e., the constant μ. We did not consider age-dependent survival here, thus the probability μ is the same for each age class. We will consider generalizations of μ in future work and note that constant survival probability has been used previously for structured population modeling of daphnids [23, 41].

Model B generalizes model A by considering a delayed effect of density on fecundity. This generalization is based on previous studies which showed that number of offspring

Model	$a(t,i)$	$b(t,i)$
A	$\alpha(i)(1-q)^{N(t)}$	μ
B	$\alpha(i)(1-q)^{N(t-\tau)}$	μ
C	$\alpha(i)(1-q)^{N(t-\tau)}$	$\mu(1-c)^{N(t)}$ if $i \leq 4$, μ if $i \geq 5$
D	$\alpha(i)(1-q)^{M(t-\tau)}$	$\mu(1-c)^{M(t)}$ if $i \leq 4$, μ if $i \geq 5$

(a) Age-dependent fecundity, $a(t,i)$, and survival probability, $b(t,i)$ in equation (1).

Parameter/ Variable	Description	Units
$p(t,i)$	Number of daphnids of age i	# of daphnids
$N(t)$	Total population size at time $t := \sum_{i=1}^{i_{max}} p(t,i)$	# of daphnids
q	Density-dependent fecundity constant	dimensionless
$\alpha(i)$	Density-independent fecundity rate	# neonates·daphnid^{-1}·day^{-1}
μ	Density-independent survival probability	day^{-1}
τ	Delay for density-dependent fecundity	days
c	Density-dependent survival constant	dimensionless
$M(t)$	Total biomass at time $t := \sum_{i=1}^{i_{max}} p(t,i)\frac{KZ_0e^{ri}}{K+Z_0(e^{ri}-1)}$	# $\cdot$ mm
K	Average maximum daphnid size (major axis)	mm
r	Average daphnid growth rate	mm/hour
Z_0	Average neonate size (major axis)	mm

(b) Parameter/Variable descriptions.

Table 1: Descriptions of models, parameters, and variables with unknown parameters $\theta = (\mu, q)$ in Models A and B and $\theta = (\mu, q, c)$ in Models C and D to be estimated.

produced by gravid female daphnids in their current cohort was unaffected by increases in population density. Instead, increased population density had an effect on subsequent cohorts [23, 41]. Since daphnids in their reproductive stage produce neonates approximately every 3 days, we bounded the time-delayed fecundity effect, τ, between 0 and 6 days.

2.1.2 Density- and age-dependent survival

We next evaluated whether density and age were important factors for modeling survival in daphnid populations. To test this, we created model C (with parameters $\theta = (\mu, q, c)$ to be estimated), which generalizes model B by including a reduced fitness for daphnids classified as juveniles in our data, i.e., less than 5 day old daphnids (see Figure 1). This generalization is based on the observation that larger daphnids consume more algae than smaller daphnids [44]. The restriction of density-dependent survival to juvenile daphnids is in agreement with previous studies which suggested that the survival of adult daphnids is not affected by competition [37]. This competitive effect is likely an important consideration for the daphnids in our population experiments, since our populations were fed a constant amount of algae each day. Indeed, previous modeling studies have suggested that daphnid survival rates would best be modeled as an age- or size-dependent function rather than as a constant [14, 24, 40, 42].

2.1.3 A density-dependent model with biomass

Lastly, we evaluated whether total biomass could more accurately capture the density-dependence of fecundity and survival than the total number of individuals in our daphnid populations. This consideration is in concordance with the generalization in model C, which relies on the observation that larger daphnids contribute more heavily to competition through resource depletion than smaller daphnids [44]. To test our hypothesis about biomass dependency, we generated Model D (again with parameters $\theta = (\mu, q, c)$ to be estimated) by replacing the total population size, $N(t)$, in model C by total biomass, $M(t)$ (see Table 1). To model total biomass, we calculated a weighted population value using a function that relates age to size. Specifically, we found that the logistic function accurately models the average size of daphnids as a function of age based on fits to individual-level experimental data (Figure 2). Consequently, we used the logistic function to weight the daphnid size in the model for the total biomass $M(t)$ (see Table 1b).

2.2 Laboratory studies

We conducted two studies in the laboratory to generate data for refining and parameterizing our mathematical model. The first study was performed at the individual daphnid level to track the baseline fecundity and growth rates in isolation, i.e., density-independent rates. The second study was performed at the population level, in duplicate, for 102 days. The individual level data was used to estimate the density-independent parameters used in our

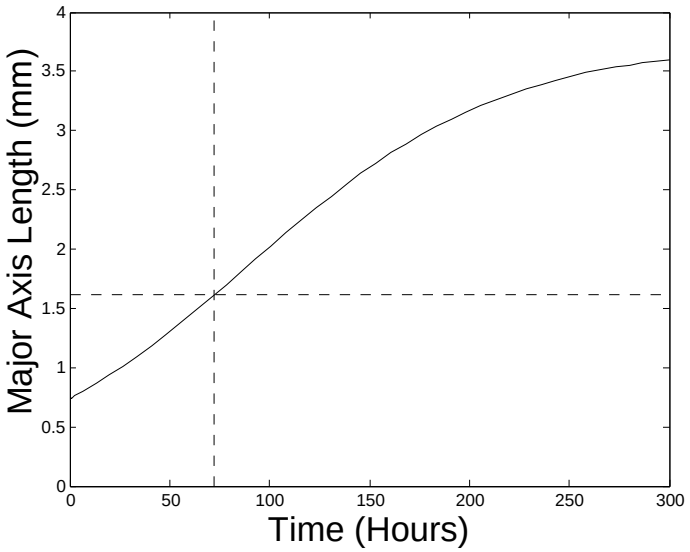

Figure 1: Calibration of the maximum size for classification of juveniles. We determined the maximum juvenile daphnid size by simulating the logistic growth curve with mean parameter values from the nonlinear mixed effects model (Figure 2, Table 2). The pore size of the mesh we used to separate juveniles from adults was 1.62 mm, and this value is plotted as a horizontal line. The vertical line gives the average daphnid age at which their major axis length is equal to the mesh pore size. Based on this calculation, we inferred that the maximum age at which daphnids can fit through the mesh was 4 days old. Thus, we chose to classify juveniles in our models as ≤ 4 days old.

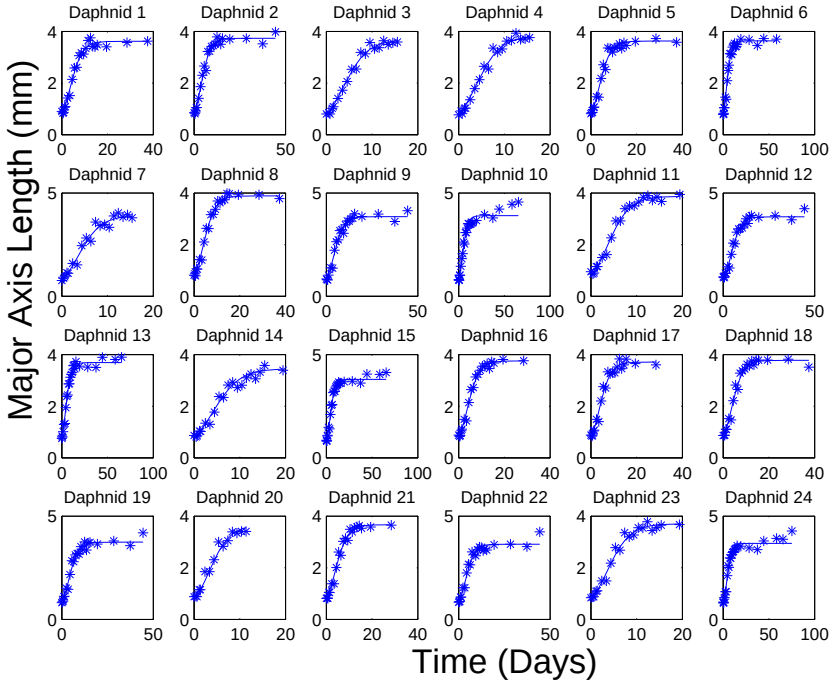

Figure 2: Results for nonlinear regression performed on individual level growth data using a logistic equation within a nonlinear mixed effects model (NLMEM). Growth data are represented by star symbols. Best model fits are drawn as lines for each individual. We collected data for thirty daphnids, but these plots show results for twenty four daphnids for which an adequate number of data was collected to fit a NLMEM. Nonlinear regression was performed using the *nlmefit* function in Matlab. We tested several models for growth, including logistic, gompertz, constant, and linear equations. Based on AIC_C values, it was determined that the logistic model provided the most accurate fit to the data. See Table 2 for estimated parameters and variances, including fixed effects and random effects.

population model. The population data was then used to estimate the remaining density-dependent parameters. Cultured daphnids were maintained using previously described protocols and conditions [48]. Cultured daphnids were kept in media reconstituted from deionized water [1]. Cultured daphnids for both studies were maintained in an incubator maintained at 20 degrees Celsius with a 16-h light, 8-h dark cycle. The daphnids used in our study came from a colony that was maintained at North Carolina State University for over 20 years (clone NCSU1 [43]).

2.2.1 Individual study

Thirty daphnids were longitudinally observed to estimate population average rates of fecundity and growth. Less than 2-h old neonates were placed individually into 50mL beakers containing 40mL of media each. Media was changed daily. Daphnids were fed daily with 7.0×10^6 cells of algae (*Pseudokirchneriella subcapitata*) and 0.2 mg (dry weight) Tetrafin$^{\text{TM}}$ fish food suspension prepared as described previously [38]. The number of neonates produced by each individual daphnid was recorded and then removed daily. Fecundity measurements were performed until no daphnids remained (74 days). The size of each individual daphnid was measured with a digital microscope (Celestron, Torrance, CA, USA) at periodic intervals until they died, starting at less than two hours old. The major axis was used to determine size, since the maximum possible length was used to classify daphnids into different size classes, i.e., juveniles and adults (see below).

2.2.2 Population study

A 102-day population study was conducted, in replicate, using *D. magna*. Two beakers containing 1L of media each were both seeded with five 6-day-old female daphnids. We note that these daphnids did not reproduce prior to the beginning of the population study. Each 1L beaker was fed twice daily (at approximately 10 a.m. and 3 p.m.) with 1.4×10^8 cells of algae (*P. subcapitata*) and 4 mg dry weight of fish food suspension. The media was changed and the number of daphnids were counted every Monday, Wednesday, and Friday through the first 40 days of the experiment and once weekly thereafter. During counting, daphnids were separated into two size classes (which we call the juvenile class and adult class) using a fine mesh net with a 1.62-mm pore size. The total number of daphnids was then counted for each size class. Importantly, we note that classification into the juvenile or adult group only defines the size of the daphnid, and does not define whether the daphnid had reached a reproductive stage.

2.3 Estimation of density-independent rates

We used data from our individual level study to estimate the density-independent fecundity rate, which we call $\alpha(i)$. We parameterized the function $\alpha(i)$ defined at age i by directly

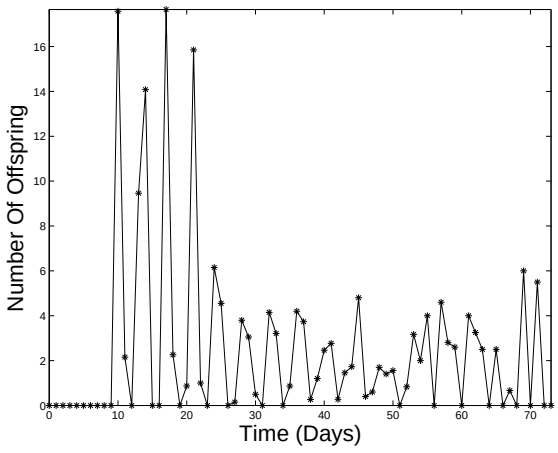

Figure 3: The number of neonates produced per female daphnid per day. Data were collected from thirty female daphnid whose birth was known to within two hours of accuracy. Daily data are represented by star symbols and connecting lines are drawn to show general trends. This data was used to parameterize the age-dependent function $\alpha(i)$ (see Table 1).

using the average number of neonates produced per daphnid per day observed in our individual level study (Figure 3).

We used the individual level growth (size) data to estimate the relationship between age and size. We considered several functional forms for $f(i)$, the average size of a female daphnid at age i, within a nonlinear mixed effects model framework and found that the logistic equation $f(i) = \frac{KZ_0e^{ri}}{K+Z_0(e^{ri}-1)}$ most accurately fit the data for individual daphnid growth (Figure 2, Table 2). Based on the mean parameter values estimated with the nonlinear mixed effects model, we inferred that the daphnids classified as juveniles in our population experiments were less than or equal to 4 days old, and that adults were greater than 5 days old (Figure 1). The function $f(i)$ was also used to replace total population size with a model for total population biomass in one of the population models we described above.

Parameter	K	r	M_0
Fixed Effect Mean Value	3.7346	0.0157	0.7333
Random Effect Variance	0.0010533	0.0048239	6.8978 x 10^{-7}

(a) Mean values and variances (random effects) estimated for the logistic equation with a nonlinear mixed effects model.

Daphnid	K	r	M_0
1	3.6148	0.0157	0.7333
2	3.7342	0.0160	0.7333
3	3.6834	0.0156	0.7333
4	3.8267	0.0156	0.7333
5	3.6262	0.0162	0.7333
6	3.6340	0.0157	0.7333
7	3.8957	0.0169	0.7334
8	3.8895	0.0154	0.7333
9	3.8556	0.0152	0.7333
10	3.9009	0.0145	0.7333
11	3.8718	0.0170	0.7334
12	3.8482	0.0148	0.7333
13	3.6902	0.0140	0.7333
14	3.4604	0.0138	0.7333
15	3.7969	0.0150	0.7333
16	3.7530	0.0158	0.7333
17	3.7092	0.0162	0.7333
18	3.7758	0.0164	0.7333
19	3.7397	0.0159	0.7333
20	3.6688	0.0178	0.7334
21	3.6662	0.0153	0.7333
22	3.6387	0.0163	0.7334
23	3.7070	0.0166	0.7333
24	3.6806	0.0147	0.7333

(b) Individual parameter estimates for each daphnid.

Table 2: Mean parameter estimates and variances along with individual daphnid parameter estimates for the logistic equation using a nonlinear mixed effects model (see Figure 2).

2.4 Parameter Estimation

Parameters were estimated from the population data using a vector ordinary least squares (OLS) framework [9, 11]. For each model, we consider a vector of parameters θ to estimate. Based on our individual level modeling, the number of juveniles and adults are given by $J(t,\theta) = \sum_{i=1}^{4} p(t,i)$ and $A(t,\theta) = \sum_{5}^{i_{max}} p(t,i)$, respectively. The corresponding observation vector is given by $\mathbf{f}(t,\theta) = [J(t,\theta), A(t,\theta)]^T$. We assumed a constant statistical error model of the form

$$\mathbf{Y}_j = \mathbf{f}(t_j, \theta_0) + \mathcal{E}_j, \quad j = 1, 2, ..., n,$$

where $\mathbf{Y}_j$ is a random variable with realizations $\mathbf{y}_j$ (i.e., the data) and $\mathbf{f}(t_j, \theta_0)$ is the model observation with the hypothesized "true" parameter vector θ_0. The error terms $\mathcal{E}_j$ are assumed independent and identically distributed (i.i.d) random variables with mean $E[\mathcal{E}_j] = 0$ and V_0 =var($\mathcal{E}_j$)=diag($\sigma^2_{1,0}, \sigma^2_{2,0}$). An estimate, $\hat{\theta}$, for the true parameter vector θ_0 is obtained by implementing an iterative algorithm (see [9] for details).

2.5 Model Comparisons

2.5.1 Model Hypothesis Testing

We used a statistical model comparison test [7, 11] to evaluate the significance in considering various components, e.g., delayed density-dependence, for models A through C. Briefly, this methodology evaluates the significance of a χ^2 statistic generated by the residual sum of squares to test the null hypothesis, H_0, that a certain parameter or set of parameters is not needed to describe the system. We note that this method requires nested models. For example, model A is "nested" in model B because model B reduces to model A when $\tau = 0$. If we can reject the null hypothesis H_0 then we conclude that the parameters in question cannot be taken equal to zero and infer that they are needed to accurately describe the data . For further details and previous applied examples of this methodology see [7, 28, 11].

2.5.2 Akaike Information Criteria

The Akaike Information Criterion (AIC) score gives an approximately unbiased form of the Kullback-Leibler Distance, or a measure of the distance between a model and the corresponding data [9]. The AIC score is used to compare the accuracy of different models to the same data set; a lower AIC score indicates higher accuracy. We note that the AIC score is applicable to more model comparisons than the χ^2 based test described above, since it does not require the compared models to be nested. The AIC score corrected for small sample size ($n/p < 40$, n = number of data points, p = number of parameters) is given by as $AIC_C = n \ln\left(\frac{RSS}{n}\right) + 2p + \frac{2p(p+1)}{n-p-1}$, where RSS is the *residual sum of squares* [9, 12]. We used the AIC_C score to compare the non-nested population models we considered, e.g., model C and model D.

2.6 Parameter Uncertainty Quantification

We calculated standard errors and 95% confidence intervals for the estimated parameters $\hat{\theta}$ using asymptotic theory, and used bootstrapping for verification. We provide a brief description of the application of these two methods here, but for more details see [9, 11].

2.6.1 Asymptotic Theory

The observation variance V_0 in the vector OLS framework using a constant statistical error model is approximated by

$$V_0 \approx \hat{V} = \text{diag}\left(\frac{1}{n-p}\sum_{j=1}^{n}[\mathbf{y}_j - \mathbf{f}(t_j,\hat{\theta})][\mathbf{y}_j - \mathbf{f}(t_j,\hat{\theta})]^T\right).$$

The resulting approximation of the covariance matrix is given by

$$\hat{\Sigma}^n = \left(\sum_{j=1}^{n} D_j^T(\hat{\theta})\hat{V}^{-1}D_j(\hat{\theta})\right)^{-1},$$

where the 2 x p matrix $D_j(\hat{\theta})$ is given by

$$D_j(\hat{\theta}) = \begin{pmatrix} \frac{\partial J(t_j,\hat{\theta})}{\partial\theta_1} & \cdots & \frac{\partial J(t_j,\hat{\theta})}{\partial\theta_p} \\ \frac{\partial A(t_j,\hat{\theta})}{\partial\theta_1} & \cdots & \frac{\partial A(t_j,\hat{\theta})}{\partial\theta_p} \end{pmatrix},$$

where $p = 2$ in Models A and B and $p = 3$ in Models C and D. Then asymptotic theory [9, 11] yields that the OLS estimator has a limiting distribution given approximately by a $\mathcal{N}(\hat{\theta}, \hat{\Sigma}^n)$ distribution.

We calculated standard errors and 95% confidence intervals [9, 11] in order to quantify the uncertainty in estimating each element of the parameter estimate $\hat{\theta}$ for our best model with vector observation $\mathbf{f}(t,\theta)$. The standard error and 95% confidence interval of the k^{th} parameter $\hat{\theta}_k$ is given by $SE(\hat{\theta}_k) = \sqrt{\hat{\Sigma}^n_{kk}}$ and $[\hat{\theta}_k - 1.96SE(\hat{\theta}_k), \hat{\theta}_k + 1.96SE(\hat{\theta}_k)]$, respectively [11].

2.6.2 Bootstrapping

Bootstrapping is implemented for an estimated parameter vector $\hat{\theta}$ by first calculating standardized residuals

$$\overline{r}_j^i = \sqrt{\frac{n}{n-p}}\left(y_j^i - f_i(t_j,\hat{\theta})\right),\ j = 1, ..., n,$$

where n is the number of data points, p is the number of parameters, $i = J$ or A represents either the adult or juvenile observation. Here, $f_J(t_j, \hat{\theta}) = J(t_j, \hat{\theta})$ and $f_A(t_j, \hat{\theta}) = A(t_j, \hat{\theta})$. Bootstrap sample points are created by sampling the standardized residuals for each observation (J or A) and adding them to the respective model solutions, either $J(t_j, \hat{\theta})$ or $A(t_j, \hat{\theta})$. We created $M = 1000$ simulated bootstrap data sets in this fashion and then conducted M inverse problems to fit the model to each of these simulated data sets. For the m^{th} simulated bootstrap data set, we then find the corresponding parameter estimate $\hat{\theta}^m$. The mean, variance, and standard errors for $\hat{\theta}$ are approximated by the following formulas [9]:

$$\hat{\theta}_{BOOT} = \frac{1}{M}\sum_{m=1}^{M}\hat{\theta}^m,$$

$$Var(\hat{\theta}_{BOOT}) = \frac{1}{M-1}\sum_{m=1}^{M}(\hat{\theta}^m - \hat{\theta}_{BOOT})(\hat{\theta}^m - \hat{\theta}_{BOOT})^T,$$

$$SE_k(\hat{\theta}_{BOOT}) = \sqrt{Var(\hat{\theta}_{BOOT})_{kk}}.$$

The 95 % confidence interval for each $\hat{\theta}_k$ is calculated as the range between the 25-th and 975-th entries in the ordered set of M parameter estimates from bootstrapping.

3 Results

3.1 Model Selection

When comparing models A and B we found that a 6 day time-delay on the effect of density on fecundity provided a significantly improved fit to the daphnid population data versus the non-delayed model for both population data sets (P = 5.029e-4, Replicate 1; P = 3.219e-3, Replicate 2, χ^2-test, Figure 4). We note that we also tested whether larger τ values could provide a more accurate fit to population data but found no significant differences in fits to the population data when using $\tau = 6$ versus $\tau = 7$ or 8 (P = .3071, Replicate 1; P = .1139, Replicate 2, χ^2-test).

We found that the inclusion of both density and age dependence in the survival probability $b(t, i)$ provided significantly improved fits to population data for one of the two replicates (P = 1.615e-1, Replicate 1; P = 3.96e-2, Replicate 2, χ^2-test). Overall, these results suggest that model C is more appropriate for modeling our daphnid populations than model B, since it describes a wider range of observed biological dynamics.

We note that we also considered other models that did not significantly increase the accuracy of the model to experimental population data (results not shown). For example, we considered models in which the density-dependent effects were of different functional

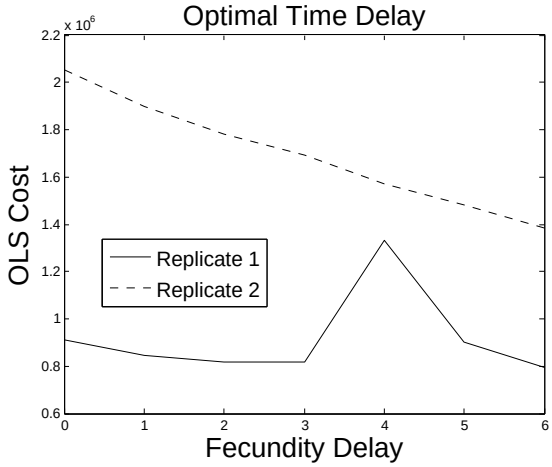

Figure 4: The ordinary least squares (OLS) cost from the inverse problem performed on model B with $\tau \in \{0, 1, ..., 6\}$ for each replicate. These results suggest that the optimal value for τ is 6 days, since it results in the smallest OLS cost.

forms. In addition, models in which all age classes (beyond 4 days old) had density-dependent survival rates did not result in significantly better fits to the population data.

Using the AIC_C score, we found that model D better described the population data from both replicates than model C. For replicate 1, the AIC_C for models C and D were 276.15 and 266.23, respectively. For replicate 2, the AIC_C for models C and D were 379.43 and 280.19, respectively. The evidence ratio, based on the calculation of Akaike weights [12, p. 74-79], for model D versus model C was 141.85 for the replicate 1 data set. The evidence ratio for model D versus model C was 3.57×10^{21} for the replicate 2 data set. These results highly suggest that model D is better than model C at representing the population data from both replicates. Hence, dependence of birth and death demographics on population density is most likely a function of a total biomass rather than the absolute number of daphnids counted regardless of size or age. See Figure 5 for fits of model D to the population data. Moreover, the parameter estimates for both replicates were strikingly similar, indicating that our validation of model D is repeatable despite the possibility of biological variability between population experiments.

3.2 Uncertainty Analysis

We quantified uncertainty in our parameter estimates for model D. Uncertainty quantification provides an estimation of the statistical confidence in each parameter for a given data set, where confidence is determined by estimating a distribution for each parameter. We calculated standard errors and 95% confidence intervals for each parameter using asymptotic theory and bootstrapping (Table 4, Figure 6). Both the results from asymptotic theory and bootstrapping support that the standard errors were low and the 95% confidence intervals were narrow for the parameter estimates in both replicates. These results indicate a high confidence that our model validation results are repeatable.

To investigate how parameter uncertainty propagates through the model solution over time, and to quantitatively assess the performance of model D, we generated a 95% confidence region for the model using Monte Carlo (MC) simulations. We sampled 1000 parameter vectors from the 95% confidence interval (C.I.) of the joint parameter distribution estimated with asymptotic theory for model D. We then generated 95% confidence regions for the number of juveniles, the number of adults, and the total population size by simulating the corresponding 1000 model solutions and plotted these along with the data and their error bars (Figure 5). We then calculated the percentage of data points with error bars that overlapped with the 95% confidence region simulations to assess the overall model performance and account for uncertainty. We found that model D matched the population data from both replicates with high accuracy for both juveniles and adults, as well as for the total population size (Table 3).

Daphnid Classification	Replicate	% Accuracy	Fraction
Juvenile	1	100 %	25/25
Adult	1	96 %	24/25
Total	1	96%	24/25
Juvenile	2	92 %	23/25
Adult	2	96 %	24/25
Total	2	96 %	24/25

Table 3: The percentage (% accuracy) and fraction of observed data points with error bars that overlapped with the 95 % confidence region for model D. Results are shown for the number of juveniles, the number of adults, and the total population size.

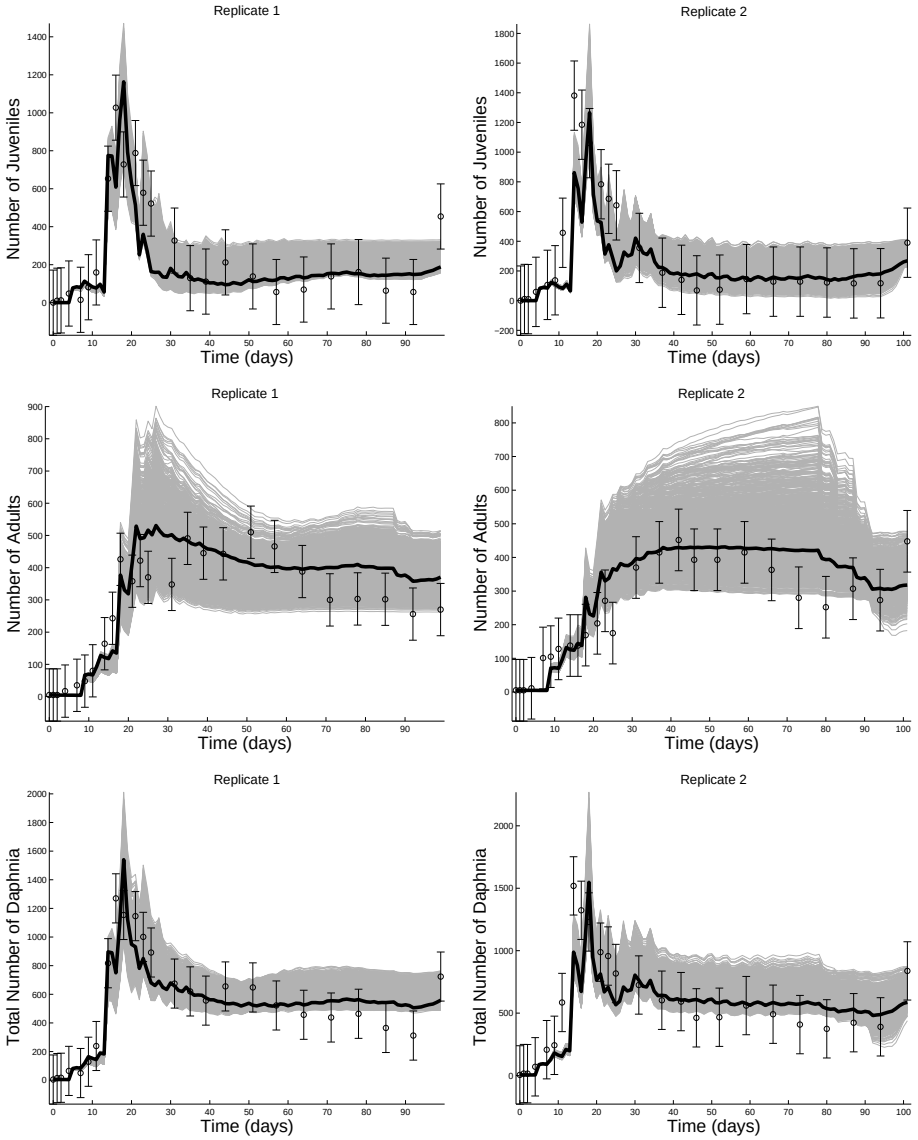

Figure 5: Results from fitting model D to juvenile and adult longitudinal population data for *D. magna*. Results are shown for juveniles (top), adults, (middle), and total population size (bottom), for replicate number 1 (left) and 2 (right). Black lines: Simulation results using the estimated parameter vector for model D. Gray lines: Simulated population model results with parameters sampled from the 95% confidence interval of the joint asymptotic distribution. The data are plotted as open circles with error bars for the estimated observation variance. The parameter values used for these plots can be found in Table 4 below.

Replicate	Parameter	Estimate	Standard Error	95 % C.I.
1	μ	9.5051×10^{-1}	1.0428×10^{-2}	$(9.2889\times10^{-1},9.7214\times10^{-1})$
1	q	1.7206×10^{-3}	1.5426×10^{-4}	$(1.4007\times10^{-3},2.0405\times10^{-3})$
1	c	1.5153×10^{-4}	2.9689×10^{-5}	$(8.9972\times10^{-5},2.1310\times10^{-4})$
2	μ	9.8559×10^{-1}	8.1785×10^{-3}	$(9.6863\times10^{-1},1.0025)$
2	q	1.3542×10^{-3}	1.7762×10^{-4}	$(9.8590\times10^{-4},1.7225\times10^{-3})$
2	c	2.8005×10^{-4}	4.1701×10^{-5}	$(1.9358\times10^{-4},3.6652\times10^{-4})$

(a) Parameter estimates, asymptotic standard errors, and asymptotic 95% confidence intervals (C.I.) for model D.

Replicate	Parameter	Estimate	Standard Error	95 % C.I.
1	μ	9.5051×10^{-1}	8.7505×10^{-3}	$(8.8922\times10^{-1},9.2551\times10^{-1})$
1	q	1.7206×10^{-3}	2.3202×10^{-4}	$(2.0358\times10^{-3},2.9980\times10^{-3})$
1	c	1.5153×10^{-4}	2.3608×10^{-5}	$(-4.8952\times10^{-5},4.8953\times10^{-5})$
2	μ	9.8559×10^{-1}	2.3660×10^{-2}	$(9.3715\times10^{-1},1.0355)$
2	q	1.3542×10^{-3}	3.2867×10^{-4}	$(6.8486\times10^{-4},2.0517\times10^{-3})$
2	c	2.8005×10^{-4}	9.7547×10^{-5}	$(8.3218\times10^{-5},4.8888\times10^{-4})$

(b) Parameter estimates, bootstrap standard errors, and bootstrap 95% confidence intervals (C.I.) for model D.

Table 4: Results from uncertainty quantification with asymptotic theory and bootstrapping for model D.

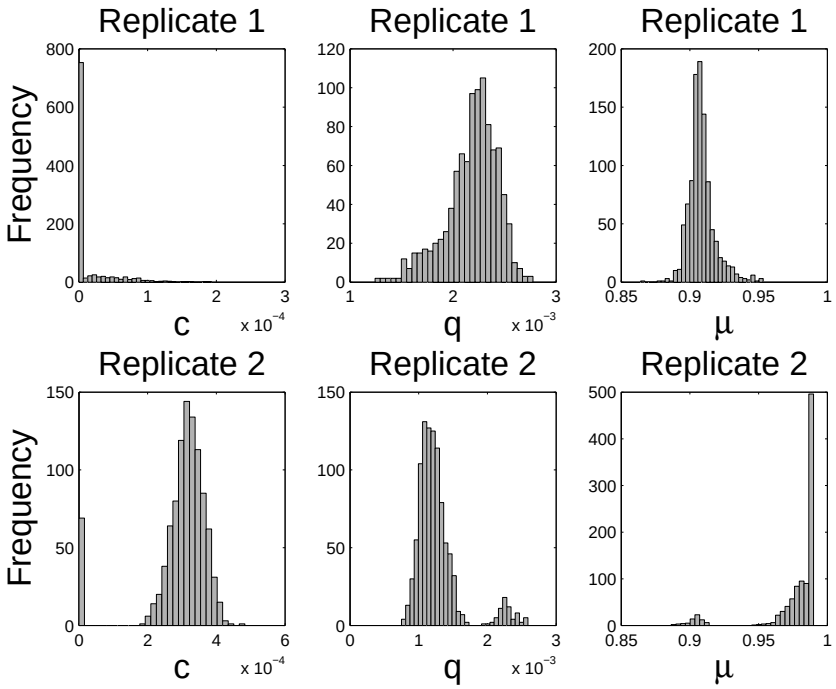

Figure 6: The parameter distributions obtained from bootstrapping for each estimated parameter (μ, q, c) and each replicate for model D.

3.3 Parameter Sensitivities

We applied a sensitivity analysis to our best validated model (model D) to understand how changes in estimated parameters governing fecundity and survival affect population size and structure. We calculated the relative time-dependent sensitivity functions for juvenile, adult, and total population size (Figure 7). Interestingly, we observed that the maximum total population size for our two replicates was achieved on day 19, dividing the population dynamics into two phases, which we call the "early phase" and the "late phase" (Figure 8). In the early phase ($\leq$ 19 days) of the population experiments, the population grows rapidly and exceeds its carrying capacity. In the late phase of the population experiments ($>$ 19 days), the total population size converges towards steady state levels as an excess juvenile population rapidly dies off or progresses to the adult stage. Dividing our sensitivity analysis between these two phases revealed that the effect of increasing fecundity or survival is both temporally and life-stage dependent (Figure 9).

We found that the juvenile, adult, and total population sizes were most sensitive to changes in μ in both the early and late phase as compared to the other estimated parameters q and c. The sensitivity analysis indicates that increasing the survival parameter μ will increase the juvenile population in the early phase and decrease it in the late phase, whereas an increased μ increases the adult population size in both the early and late phase. Although increased survival increases the total population size in the early phase, the late phase is much less sensitive. These findings suggest that increases in the survival parameter μ will cause a shift in the population distribution towards the adult stage and that this shift mainly occurs during the early phase of population growth.

Our sensitivity analysis indicates that increasing q, the effect of density on fecundity, has a greater effect in the late phase of the population experiment than in the early phase for the juvenile, adult, and total population size. This result is expected, since a lower fecundity rate should lead to lower population sizes overall and within specific life stages. We hypothesize that the late phase is more heavily influenced by a decreased density-dependent fecundity rate than the early phase because of the time delayed effect. If so, this would imply that most of the offspring in the early phase are produced by female daphnids whose fecundity has not yet been effected by density.

Lastly, our sensitivity analysis indicates that increasing c, the effect of density on the survival of juveniles, leads to lower numbers of juveniles and adults, and a lower total population size in the early phase. This relationship is more pronounced in the late phase for both the number of adults and total population size. Unexpectedly, our sensitivity analysis indicates that increasing the parameter c can cause the number of juveniles to increase during the late phase of the population experiments.

Taken together, these findings suggest that a higher density-dependent juvenile survival probability can cause a shift towards juveniles in the equilibrium age distribution of daphnid populations, even though the total population size decreases overall. Our results highlight the importance of mathematical modeling to understand non-intuitive temporal shifts in

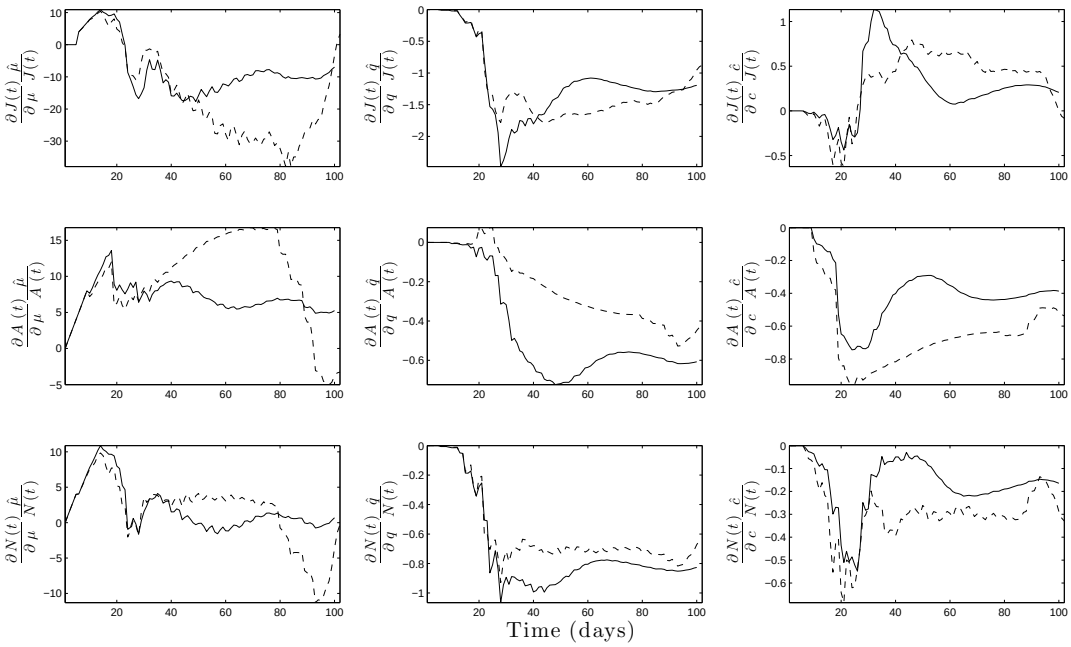

Figure 7: The relative time-dependent sensitivities for juveniles, adults, and the total population with respect to each of the estimated parameters (μ, q, c) for model D. Sensitivities were calculated for the number of juveniles $J(t)$ (top row), the number of adults $A(t)$ (middle row), and the total population size $N(t)$ (bottom row). The left column corresponds to μ, the middle column to q, and the right column to c. Solid lines: Replicate 1. Dashed lines: Replicate 2.

the age distribution of daphnid populations that may occur under environmental conditions that increase competition, e.g., if the amount of algae decreases.

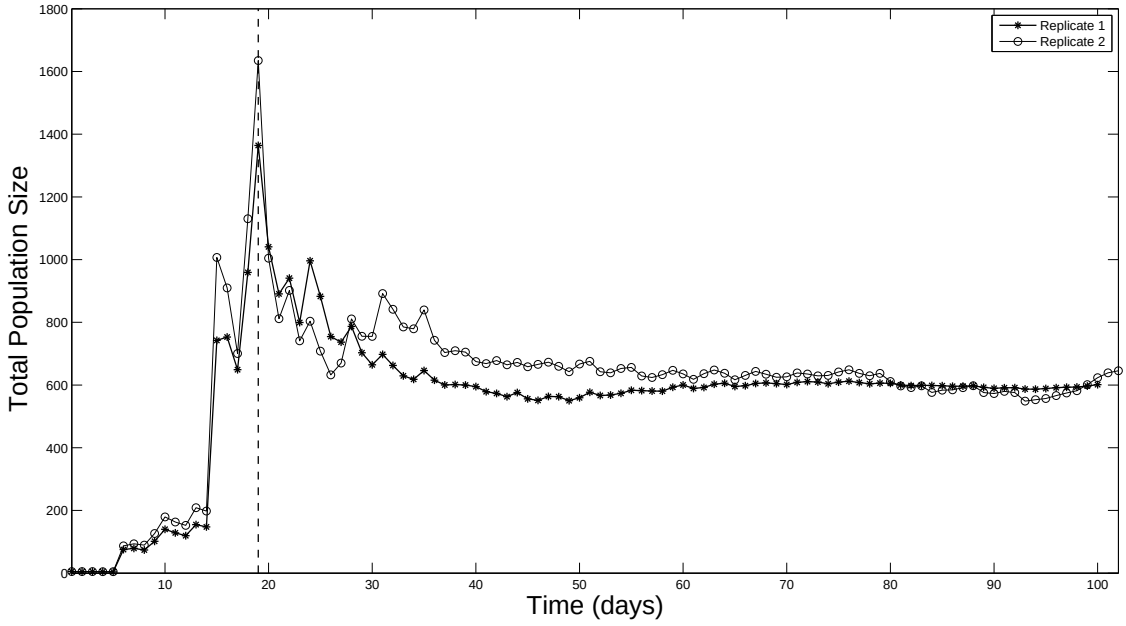

Figure 8: Longitudinal data for the total population size for two population replicates. The vertical dashed line is at 19 days, and shows the division between the early phase and late phase dynamics.

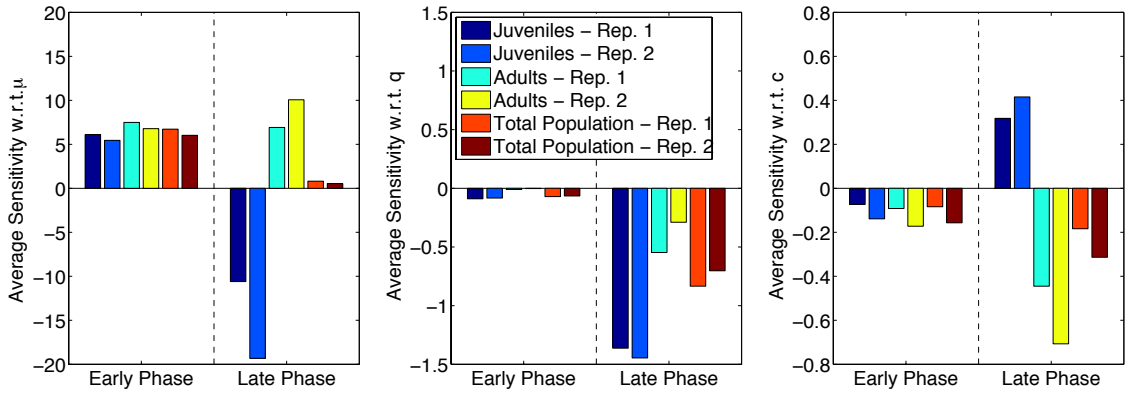

Figure 9: The average of the relative sensitivities during the early and late phases for juvenile, $J(t)$, adult, $A(t)$, and total population, $N(t)$, counts with respect to the survival parameter, μ, the effect of density on fecundity, q, and the effect of density on survival, c. Sensitivities are divided between the early phase of the population experiments (before the peak size is reached on day 19) and the late phase (after day 19).

4 Conclusions and Discussion

We tested several hypotheses concerning the significance of several biological assumptions in describing daphnid populations with a structured population model. One assumption we evaluated, delayed density-dependent fecundity, had been suggested previously [23, 41]. Importantly, this hypothesized mechanism was not quantitatively verified due to a lack of statistical comparison tools at the time they were proposed. We applied a χ^2 based model comparison test and found strong statistical evidence for a time delay in density dependent fecundity. We also found statistical evidence for the assumption that intraspecific competition mainly affects juvenile daphnids, previously suggested in [14, 24, 40, 42]. Lastly, we determined that the effect of density on daphnid demographics is more accurately modeled as a function of total biomass, rather than total population size [23, 44]. Our findings indicate that the assumptions we investigated can improve the accuracy of future daphnid population modeling efforts and may provide increased accuracy in other daphnid models which may not have considered all of these assumptions [18, 19, 21, 22, 23, 42].

We found that parameterizing the density-independent components of demographic rates with individual level data enabled the estimation of density-dependent parameters from aggregate structured population data. The most complex density-independent component that we discovered was for daphnid fecundity (Figure 3). Our data revealed a clear periodic pattern in the timing of offspring production in which daphnids begin releasing neonates at 9-days-old. Notably, the maximum offspring production rate is significantly higher in the first 4 broods than in subsequent broods ($P = 0.0011$, Mann-Whitney U-test). To the best of our knowledge, fecundity oscillations with a consistent frequency and time-dependent amplitude has not previously been observed for daphnids. We note that without employing individual level time-dependent fecundity data, our attempts to fit daphnid population data gave extremely poor results (data not shown). We suspect that the collection of similarly precise individual-level data will be necessary to parameterize structured models from field data of daphnid populations. For example, daphnids could be sampled in the field and cultured/observed under experimental conditions similar to their natural environment. Alternatively, one may be able to employ computational methods designed to estimate time-dependent rates from aggregate data alone [2, 3, 4, 5, 6, 8, 9, 10]. However, these methods have only been previously applied to density-independent structured population models, and thus they remain largely untested and underdeveloped in density-dependent scenarios.

An underlying challenge in performing hazard assessments is to generate a highly repeatable baseline control for comparison. For our best validated model (Model D), the parameter estimates, uncertainty quantification, temporal variations in sensitivity patterns, and overall degree of accuracy to the data were all extremely similar between replicates (Figures 5 and 9, Tables 3 and 4). These results highlight the need for comprehensively evaluating biological assumptions about daphnid populations grown under non-stressed en-

vironmental conditions, i.e., the control case. Our results also suggest the need for further improvement, since Model D underestimated the early phase ($\leq$ 19 days) growth rate and the time at which the peak size was reached for the juvenile population in the second replicate. One possible adjustment that may increase the accuracy of model D is to incorporate an age-dependent daphnid survival probability. From our sensitivity analysis, we infer that increasing the juvenile survival probability will likely remedy the underestimation of the early phase growth rate (Figure 9). For simplicity, we assumed a constant parameter μ for the density-independent survival probability in the modeling efforts reported here; however, this assumption is a current focus of our ongoing investigations.

Acknowledgements

This research was supported in part by the National Institute of Allergy and Infectious Diseases under grant number NIAID R01AI071915-10, in part by the Air Force Office of Scientific Research under grant number AFOSR FA9550-12-1-0188, in part by the National Science Foundation under Research Training Grant (RTG) DMS-1246991, NSF Undergraduate Biomathematics grant number DBI-1129214, NSF grant number DMS-0946431, in part by the EPA under US EPA STAR grant RD-835165, and in part by the NIEHS under training grant ES7046.

References

[1] W.S. Baldwin, G.A. LeBlanc, Identification of multiple steroid hydroxylases in *Daphnia magna* and their modulation by xenobiotics, Environ. Toxicol. Chem. 13 (1994): 1013-1021.

[2] H.T. Banks, L.W. Botsford, F. Kappel, C. Wang, Modeling and estimation in size structured population models, LCDS-CCS Report 87-13, Brown University. *Proc. 2nd Course on Mathematical Ecology*, (Trieste, December 8-12, 1986) Word Press (1988), Singapore, 521-541.

[3] H.T. Banks, J.L. Davis, S.L. Ernstberger, S. Hu, E. Artimovich, A.K. Dhar, Experimental design and estimation of growth rate distributions in size-structured shrimp populations, Inverse Probl. 25 (2009): 095003.

[4] H.T. Banks, J.L. Davis, S.L. Ernstberger, S. Hu, E. Artimovich, A.K. Dhar, C.L. Browdy, A comparison of probabilistic and stochastic formulations in modeling growth uncertainty and variability, J. Biological Dynamics 3 (2009):130-148.

[5] H.T. Banks, J.L. Davis, S. Hu, A computational comparison of alternatives to including uncertainty in structured population models, In *Three Decades of Progress in Systems and Control*, (X. Hu, et. al., eds.), Springer, New York, 19-33 (2010).

[6] H.T. Banks, B.G. Fitzpatrick, Estimation of growth rate distributions in size structured population models, Quarterly of Applied Mathematics, 49 (1991):215-235.

[7] H.T. Banks and B.G. Fitzpatrick, Statistical methods for model comparison in parameter estimation problems for distributed systems, Journal of Mathematical Biology 28 (1990): 501-527.

[8] H.T. Banks, B.G. Fitzpatrick, L.K. Potter, Y. Zhang, Estimation of probability distributions for individual parameters using aggregate population data, In *Stochastic Analysis, Control, Optimization, and Applications*, (W. McEneaney, G. Yin, and Q. Zhang, eds.), Birkhauser, Boston, (1989).

[9] H.T. Banks, S. Hu, W.C. Thompson, Modeling and Inverse Problems in the Presence of Uncertainty, CRC Press, New York, 2013.

[10] H.T. Banks, K. Kunisch, Estimation Techniques for Distributed Parameter Systems, Birkhausen, Boston, 1989.

[11] H.T. Banks, H.T. Tran, Mathematical and Experimental Modeling of Physical and Biological Processes, CRC Press, New York, 2009.

[12] K.P. Burnham, D.R. Anderson, Model Selection and Inference: A Practical Information-Theoretic Approach (2nd edition), Springer-Verlag, New York, 2002.

[13] H. Caswell, Matrix Population Models: Construction, Analysis, and Interpretation (2nd edition), Sinauer, Sunderland, MA, 2001

[14] M. Cleuvers, B. Goser, H.T. Ratte. Life-strategy shift by intraspecific interaction in *Daphnia magna*: change in reproduction from quantity to quality, Oecologia 110 (3) (1997): 337-345.

[15] D.T. Crouse, L.B. Crowder, H. Caswell, A stage-based population model for loggerhead sea turtles and implications for conservation, Ecology 68 (1987): 1412-1423.

[16] D. Doak, P. Kareiva, B. Klepetka, Modeling population viability for the desert tortoise in the western Mojave Desert, Ecol. Appl. 4 (1994), 446-460.

[17] D.F. Doak, W.F. Morris, Quantitative Conservation Biology: Theory and Practice of Population Viability Analysis, Sinauer, Sunderland, MA, 2002.

[18] M. El-Doma, A size-structured dynamics model of *Daphnia*. Applied Mathematics Letters 25 (2012): 1041-1044.

[19] M. El-Doma. Stability analysis of a size-structured population dynamic model of *Daphnia*, International Journal of Pure and Applied Mathematics 70 (2) (2011): 189-209.

[20] P. Endels, H. Jacquemyn, R. Brys, M. Hermy, Rapid response to habitat restoration by the perennial *Primula veris* as revealed by demographic monitoring. Plant Ecol. 176 (2005): 143-156.

[21] R.A. Erickson, S.B. Cox, J.L. Oates, T.A. Anderson, C.J. Salice, K.R. Long. A *Daphnia* population model that considers pesticide exposure and demographic stochasticity, Ecological Modeling, 275 (2014):37-47.

[22] J.Z. Farkas, T. Hagen, Linear stability and positivity results for a generalized size-structured *Daphnia* model with inflow, Applicable Analysis 86 (2007): 1087-1103.

[23] P.W. Frank, Prediction of population growth form in *Daphnia pulex* cultures, The American Naturalist 94 (878) (1960): 357-372.

[24] P.W. Frank, C.D. Boll, R.W. Kelly, Vital statistics of laboratory cultures of *Daphnia pulex* as related to density, Physiological Zoology 30 (4) (1957): 287-305.

[25] M. Fujiwara, H. Caswell, Demography of the endangered North Atlantic right whale, Nature 414 (2001): 537-54.

[26] C. Guisande, Reproductive strategy as population density varies in *Daphnia magna* (Cladocera), Freshwater Biology 29 (3) (1993): 463-467.

[27] D.G. Hole, M.J. Whittingham, R.B. Bradbury, G.Q.A. Anderson, P.L.M. Lee, J.D. Wilson, J.R. Krebs, Widespread local house-sparrow extinctions. Nature 418 (2002): 931-932.

[28] T. Huffman, K. Link, J. Nardini, L. Poag, K.B. Flores, H.T. Banks, B. Blasco, J. Jungfleisch, J. Diez, A mathematical model of RNA3 recruitment in the Brome Mosaic Virus replication cycle, International Journal of Pure and Applied Mathematics 89 (2) (2013): 251-274.

[29] W.L. Kendall, J.E. Hines, J.D. Nichols, Adjusting multistate capture-recapture models for misclassification bias: Manatee breeding proportions, Ecology 84 (2003): 1058-1066.

[30] W. Lampert, Response of the respiratory rate of *Daphnia magna* to changing food conditions, Oecologia 70 (4) (1986): 495-501.

[31] G.A. LeBlanc, C.V. Rider, An integrated addition and interaction model for assessing toxicity of chemical mixtures, Toxicological Sciences 87 (2) (2005):520-528.

[32] G.A. LeBlanc, Y.H. Wang, C.N. Holmes, G. Kwon, E.K. Medlock, A transgenerational endocrine signaling pathway in crustacea, PLoS One 8 (4) (2013): e61715.

[33] P.H. Leslie, On the use of matrices in certain population mathematics, Biometrika 33 (3) (1945): 183-212.

[34] J.W. MacArthur, W.H.T. Baillie, Metabolic activity and duration of life. I. Influence of temperature on longevity in *Daphnia magna*, Journal of Experimental Zoology, 53 (2) (1929) :221-242.

[35] F. Martinez-Jeronimo, R. Villasenor, G. Rios, F. Espinosa, Effect of food type and concentration on the survival, longevity, and reproduction of *Daphnia magna*, Hydrobiologia 287 (1994): 207-214.

[36] National Institutes of Health. *Daphnia. Model Organisms for Biomedical Research.* http://www.nih.gov/science/models/daphnia/.

[37] W.E. Neill. Experimental studies of microcrustacean competition, community composition and efficiency of resource utilization, Ecology 56 (1975): 809-826.

[38] A.W. Olmstead, G.A. LeBlanc, The environmental-endocrine basis of gynandromorphism in a crustacean, International Journal of Biological Sciences 3 (2007): 77-84.

[39] B. Pietrzak, M. Grzesuik, A. Bednarska, Food quantity shapes life history and survival strategies in *Daphnia magna* (Cladocera), Hydrobiologia 643 (2010): 51-54.

[40] K. G. Porter, J. D. Orcutt Jr., J. Gerritsen, Functional response and fitness in a generalist filter feeder, *Daphnia magna* (Cladocera: Crustacea), Ecology 64 (4) (1983) 735-742.

[41] D.M. Pratt, Analysis of population development in *Daphnia* at different temperatures, The Biological Bulletin 85 (2) (1943): 116-140.

[42] T.G. Preuss, M. Hammers-Wirtz, U. Hommen, M.N. Rubach, H.T. Ratte, Development and validation of an individual based *Daphnia magna* population model: The influence of crowding on population dynamics, Ecological Modeling 220 (2009): 310-329.

[43] C.V. Rider, T.A. Gorr, A.W. Olmstead, B.A. Wasilak, G.A. LeBlanc, Stress signaling: coregulation of hemoglobin and male sex determination through a terpenoid signaling pathway in a crustacean, Journal of Experimental Biology 208 (2005): 15-23.

[44] J.H. Ryther. Inhibitory effects of phytoplankton upon the feeding of *Daphnia magna* with reference to growth, reproduction, and survival, Ecology 35 (4) (1954): 522-533.

[45] J.D. Stark, J.E. Banks, Selective pesticides: are they less hazardous to the environment?, Bioscience 51 (2001), 980-982.

[46] D.M. Thomson, Matrix models as a tool for understanding invasive plant and native plant interactions, Conserv. Biol. 19 (2005): 917-928.

[47] J.R. Vonesh, O. De la Cruz, Complex life cycles and density dependence: assessing the contribution of egg mortality to amphibian declines, Oecologia 133 (2002): 325-333.

[48] Y.H. Wang, G. Kwon, H. Li, G.A. LeBlanc, Tributyltin synergizes with 20-hydroxyecdysone to produce endocrine toxicity, Tox. Sci. 123 (2011): 71-79.

[49] H.Y. Wang, A.W. Olmstead, H. Li, G.A. LeBlanc. The screening of chemicals for juvenoid-related endocrince activity using the water flea *Daphnia magna*, Aquatic Toxicology 74 (2005):193-204.

[50] U. Wennergren, J.D. Stark, Modeling long-term effects of pesticides on populations: beyond just counting dead animals, Ecol. Appl. 10 (2000): 295-302.

[51] P.H. Wilson, Using population projection matrices to evaluate recovery strategies for Snake River Spring and Summer Chinook salmon, Conserv. Biol. 17 (2003): 782-794.

[52] S.N. Wood, Obtaining birth and mortality patterns using structured population trajectories, Ecolog. Monogr. 64 (1994): 23-24.